Research article

Synthesising graphene from plastic waste and its use with asphalt

Abdulrahman Alsaid *, Goktug Tenekeci

Civil Engineering Department Cyprus International University, 99258, Nicosia, North Cyprus, Turkey

A B S T R A C T

The global increase in the plastic waste has resulted in significant pollution increase which causes significant damage to the environment. There is an urgent need for waste management practices such as recycling to ensure sustainable development and decreasing the impact of plastic waste on the environment. The production of new materials such as graphene are associated with high cost, and there have been research efforts to develop cost effective alternative sources of graphite. considerable research has been carried out on investigating the application of homo polypropylene in asphalt construction. successful applications of this will ensure recycling and reduce waste footprint of plastic. The paper presents a proposed method of synthesising graphene from plastic waste and talc at 80 %, and 20 % of that after many experiments. Graphene was monitored at (002). (100). (004) peaks at $2\theta = 26.8°$, 42°, with 53 successive physical tests conducted to determine the quality of the graphene produced. The experiments carried out resulted in a successful production of a 98 % pure material. The synthesised graphene was then combined with asphalt using different ratios of weight: 2 %, 6 %, 8 %, and 10 % to test the physical properties of the combination. The results were compared with no graphene usage, the findings validated the findings of similar studies which demonstrate at 6 % ration combination with graphene the asphalt provides better results than without graphene. Also, testing at alternative forces of 6.5 psi and 13 psi at temperatures of 25, 40 and 60, the results showed a noticeable improvement. All tests showed better results in creep and tensile strength. It is concluded that there is a proofed concept to follow this approach to recycle waste plastic in ample ways to reduce the footprint of waste.

1. Introduction

This study is carried out on the synthesis of graphene from waste sources, plastic waste and talc is used as an alternative material in the production of graphene. This is motivated by efforts of finding cost efficient methods of producing graphene which conventionally has a costly production, and contributing to efforts of environmental sustainability through recycling of waste. The synthesised graphene in this study was applied to asphalt as a modified material, its effect was studied to determine how much ratio of the synthesised graphene on the asphalt is more efficient.

Asphalt pavement is the predominant global road construction method because of its ease of production and its efficiency in facilitating transportation. asphalt is generally considered as a material that is easy to maintain, which also contributes to its widespread adoption in road construction. Also, the ageing of asphalt pavements significantly depends on the strength factor of the used asphalt binder materials [1]. non-carbon materials such as graphene, carbon nanotubes, and carbon nanofibers have seen significant

---

research attention especially in nanotechnology research. Graphene is a small and lightweight substance that is also chemically stable, graphene has excellent optical, thermal, mechanical, and electrical properties. The properties of graphene have made a suitable material in electronic devices and polymer chemistry. Graphene is beginning to be applied as an industrial construction material, its applications include use as a binder filler. graphene has a potential of delivering significant material performance due to its properties [2–6]. graphene is a two-dimensional material that consists of a single layer of carbon atoms arranged in a hexagonal honeycomb structure as illustrated in Fig. 1.

Graphene is the thinnest known material, and is also among the strongest known materials. It has high conduction properties that are superior to most materials. It is transparent in nature, but it is densely bound together to a point where it does not allow even an atom to pass through it. Hence, graphene has been a material of significant scientific interest [7]. Despite its flexibility properties, graphene is 300 times tougher than steem, and can stretch 20 % over its original length [8]. Graphene has potential applications in many construction scenarios, and its high demand is imminent in the future. In the field of asphalt development, reports have been forwarded on the application of graphene as a pavement material with good UV resistance and physical characteristics [9–15]. Even though industrial graphene and nano carbon are characterised as the same carbon materials, they have significantly different characteristics, and the reduction in the cost of production of graphene will ensure a wider adoption of graphene because of its superior performance. The reduction of the amount of additives in asphalt improves the performance because it makes it difficult to impair. successful development of asphalt composite materials by incorporating graphene has been achieved, where asphalt emulsion is used as the binding agent [16–21]. The global increase in population implies there is a direct increase in traffic volume, this increase results in a requirement of a high efficient materials for pavements. researchers have approached this problem by trying several mixtures of asphalt in an attempt to make it both more effective and efficient in all climates. Since the advent of graphene in 2004, many researchers have approached the application of graphene in asphalt and concrete mixtures. The application of graphene as a mixture has shown significant performance improvement with regards to tensile strength, durability, and hydration [22–26]. This has led to more research efforts to find feasible industrial applications of graphene, and its applications as an alternative material [27].

1.1. Problem statement

Plastic waste is considered one of the largest sources of environmental pollution, efforts are being made to use such waste in recycling. The graphene widely used industrially are considered high cost because of their associated cost of production. The high applicability of graphene and its performance qualities has created a need of finding cost effective methods of producing the material. Hence, this research's aim at production of graphene through waste recycling and ensuring environmental sustainability. This research aims to approach the plastic waste through repurposing it for the production of graphene to provide cost efficient graphene production and contribute to sustainable development. This research focuses on contributing to the synthesis of graphene and its application in the context of asphalt production [28–31]. The use of graphene in asphalt mixture has been reported in enhancing flexibility and thermal sensitivity in asphalt [32]. The production of asphalt is relatively expensive, and with its constant demand it gets even more expensive to produce standard asphalt mixtures [33]. The aim of this research towards recycling plastic for graphene production is to ensure the significant impact of plastic on the environment is mitigated while producing graphene. The impact of plastic on the environment is significantly detrimental and critically contributes to the climate change trend [34,35].
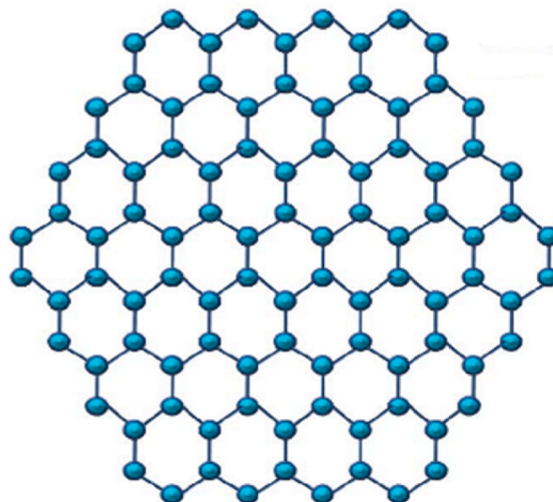

Fig. 1. Honeycomb structure of graphene.

1.2. Study contribution

Plastic waste continues to be a significant challenge on environmental sustainability and the deterioration of the environment. The formulation of adequate methods for the recycle and reuse of plastic waste continues to challenge the research and industrial sectors across the globe. Graphene as a material has many useful applications in the current industrial sphere but is significantly limited in widespread applications due to its relatively high cost. The research gap this study aims to address is the efficient recycling and reuse of plastic waste to produce cost efficient graphene materials which can be applied to asphalt construction. The contributions of this study can be highlighted as follows:

- The study proposes a novel approach for the treatment of plastic waste for the production of graphene materials.
- The proposed method of graphene synthesis in this study results in a graphene with enhanced properties and high purity compared to raw graphene.
- The synthesised graphene was used to realise an optimal asphalt mixture effective for the asphalt 40–50 standard.

This article presents a novel approach for the treatment of plastic waste towards the production of high grade graphene materials. The research uses plastic bottle waste and talc to produce graphene with high purity and enhance properties relative to raw graphene. The proposed method of this research demonstrates a novel contribution to the reuse of plastic and the production of graphene. The proposed methodology uses synthetic graphene for the modification of asphalt mixtures. several mixture proportions were used and tested to realise the optimal mixture proportion. The properties of the synthetic graphene are tested using Marshall design method, creep, durability, and tensile strength. findings of the research indicate a potential application of plastic waste in upcycling and production of graphene for use in asphalt pavement material.

2. Materials and methods

The asphalt mixture in this study uses aggregates of stone grains with graded sizes ranging from 0.075 to 50.0 mm. The aggregate contains coarse, fine and powder aggregates. The study uses asphalt binder of petroleum origin with specific temperature and environmental treatment conditions for the Asphalt 40–50 standard. Additives and improvers are used to improve the asphalt binder adhesion to the aggregate to prevent oxidation and scale.

The study also carries out Marshall l method using the Marshall l method test standard which is outlined as follows. Aggregate is dried to rid it of all moisture. Aggregate is separated into volumetric portions to match sieves of the hot funnel mixer. This study considers sieving twice to reach precise gradation. Determining the proportions of mixing different volumetric parts within specified limits. Heating the graded aggregate with the asphalt binder reaching temperatures to reduce viscosity for asphalt to reach around 170 +-30 cp. Mixing the aggregate samples with different proportions of asphalt binder. This study uses a difference in proportion of 0.5 %.
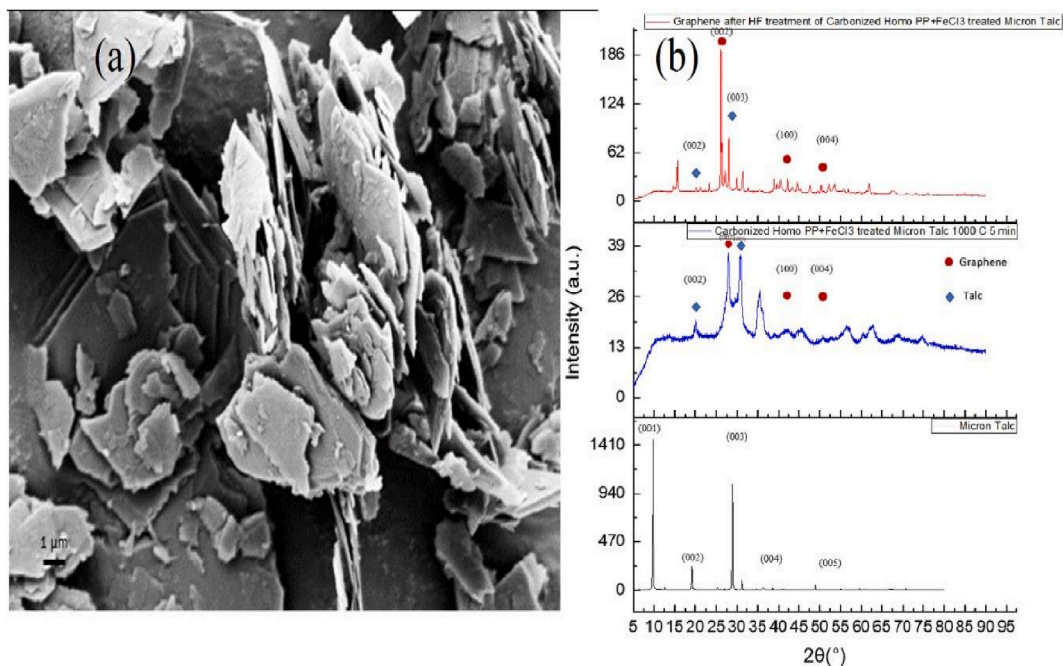

Fig. 2. (a) illustrates the synthesised graphene layers while **(b)** introduces X-ray Diffraction (XRD) peaks: (002). (100). (004) peak at 2 θ = 26.8°, 42°, and 53°

Mixed samples are placed in hot standard moulds to undergo flattening and ramming using the Marshall hammer according to the viscosity of the asphalt binder specifications; 280 +-20 cp. Samples are removed from moulds and allowed to ripen for 12 h. Samples are immersed in water, and for calculation of the volumetric properties the samples are heated at 60 °C for 2 h. Then the Marshall device is used to check the flow and stability of the samples.

The study also includes asphalt link tests which include flash point test done for safety reasons. Rolling thin film test carried out to simulate ageing at high temperature and kinetic energy relative to construction processes. The applications of pressure ageing vessels to simulate the ageing process relative to service of asphalt. Bending beam rheometer (BBR) which is used to simulate creep under tensile stress at lower temperatures. The BBR test is applied to aged asphalt binder placed in the oven and pressure vessel, this enables tests on indication of heat shrinkage and crack resistance.

2.1. Materials

This research uses bitumen 40–50 with a standard grade penetration of bitumen ASTM D946M. Fig. 2 illustrates the Scanning Electron Microscopy (SEM) images of graphene produced from directly carbonised 80 % plastic waste (Homo pp) and 20 % fine talc for a period of 5 min at a temperature of 1000° C using a thermokinetic mixer. Diffraction (XRD) peaks (002), (100), and (004) are Miller indices that refer to the different planes of the crystal lattice of the synthesised graphene. These Miller indices represent the orientation and spacing of the graphene layers.

2.2. Experiments

2.2.1. Graphene synthesis from plastic waste and talc

To obtain graphene and carbon nanoparticles growth, a surface activation of talc was done using various sizes before determining which to mix with the plastic waste. The compounds were prepared by adding iron (III) chloride ($FeCl_3$) treated talc and oxalic acid to treat the polymer, and subjected to thermal treatment. The application of oxalic acid for treating polymers and the activation of the talc in our experiments is to enable us to obtain 2D and 3D graphene structures [50]. The thermal treatment of the compound resulted in the formation of graphene and carbon nanoparticles throughout the carbonization process using carbon content in the polymer. depending on the size of the talc and the structure of the polymer; aliphatic or aromatic, the sizes of the carbon nanoparticles on the surface of talc substrate can be controlled. Figs. 3–5 illustrate the scheme for the production of graphene and carbon nanoparticles [36].

Thermokinetic mixer is used for the production of talc filled thermoplastic compounds. The talc content for the production of talc filled compound is set at 20 %, and the same ratio is applied for all compounding processes. Both treated and surface activated talc with iron oxalic are mixed using a PP at the speed of 4000–4500 revolutions per minute (rpm) at 180 °C. This study carried out planned experiments for optimum carbonization temperature and time, where talc is used directly without surface activation. Fig. 6a illustrates the XRD patterns of carbonization experiments using 20 % fine talc plus homopolymer polypropylene. Three different heat treatments are carried out in an argon atmosphere at 750 °C and 800 °C for 15 min and 1000 °C for 5 min.

A close look at the changes in XRD patterns does not reveal any change in the structure of talc at 750 °C and 800 °C. However, the process performed at 1000 °C revealed that the planar structure of the talc has changed, with observed shifts and the formation of (002), (001) and (004) peaks that belong to graphene. Similarly, due to the abundance of oxygen groups in graphene oxide, the (001) peak is also detected, and XRD peaks of (002) and (004) are also seen in reduced graphene oxide [10]. In line with the results, experiments were carried out in the subsequent carbonization processes under 1000 °C and 5 min heating time and argon atmosphere. In Fig. 6b, TGA curves of hybrid fine talc additives obtained from the carbonization process at different temperatures and times are given. Hybrid graphene with talc additive produced from carbon source from homopolymer polypropylene (PP), which is heated treated at 1000 °C for 5 min, shows a very stable thermal behaviour.

In Table 1 all the physical properties of this type of asphalt are listed, the graphene that was used in this research is graphene that was synthesised from plastic waste and talc. Table 2 shows the physical properties for synthesised graphene.

2.2.2. Functionalization and characterization of talc surface

Oxalic acid and $FeCl_3$ were used for the activation of talc, 0.5 M $FeCl_3$ solution was prepared for the functionalization of Micron
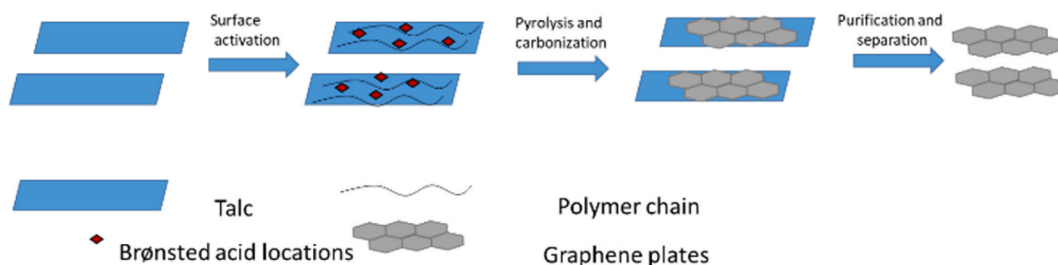

Fig. 3. Production scheme of growth of 2-D graphene plates on the talc surface by using **waste polymers.**
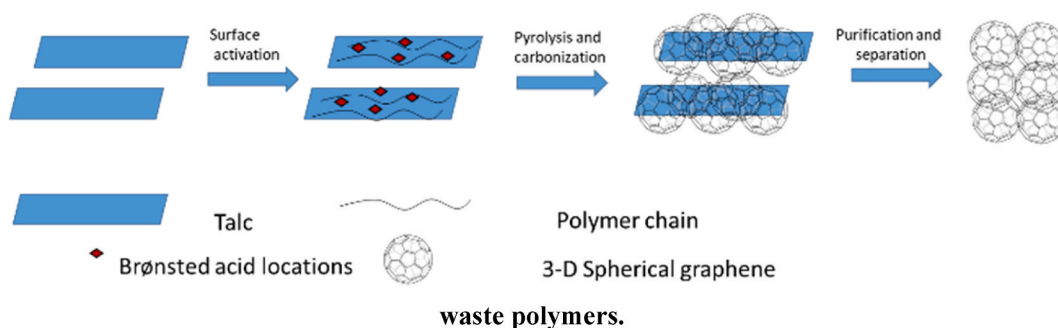
waste polymers.

Fig. 4. Production scheme of growth of 3-D spherical graphene structures on the talc surface by using waste polymers.
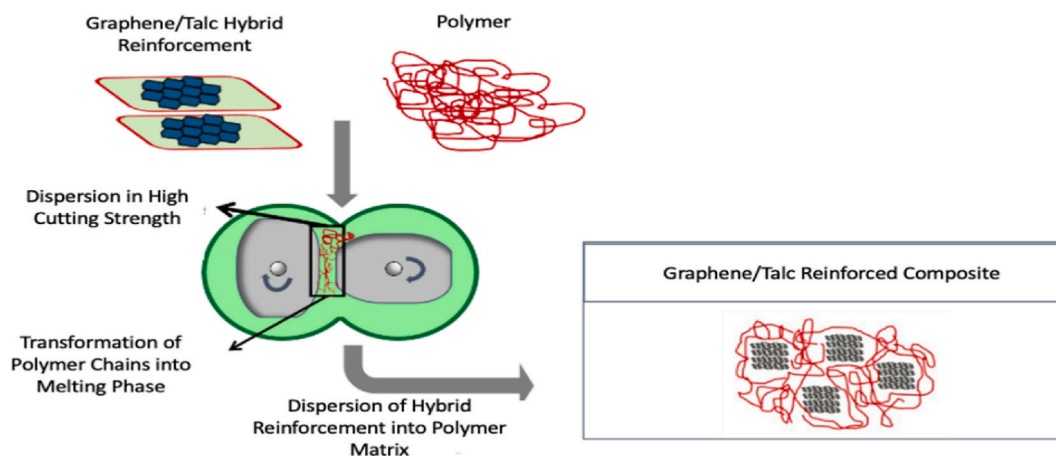

Fig. 5. 20 wt % Talc was mixed with Plastic by Thermokinetic mixer and then carbonization was performed at 1000 °C for 5 min.

Talc with iron. Then 30 g talc was mixed in 500 ml $FeCl_3$ solution at 80 °C for 24 h under reflux. Then, the filtration process was applied, and the material obtained was washed several times with distilled water. A similar study has been performed with oxalic acid as well. After mixing 13.64 g of oxalic acid ($C_2H_2O_4$) (CAS: 144-62-7) in 300 ml of distilled water, 20 g of talc was added. The prepared solution was stirred under reflux at 80 °C for 24 h. All the materials obtained were dried in the oven at 80 °C for 24 h. Characterization analyses of the talc surface were performed with Fourier Transform Infrared Spectroscopy (FTIR), X-ray diffractometer (XRD) and Thermogravimetric analyser (TGA).

2.2.3. Physical property tests on graphene

In this study, detailed analysis of the graphene, talc hybrid additive produced from Fe treated talc was made. The talc was mixed with 20 % homoPP at 4000–4500 rpm at 180 °*C* with a thermokinetic to produce a compound. Heat treatment was applied at 1000 °*C* for 5 min. The hybrid graphene/talc additive was mixed with hydrofluoric acid (HF, 20 % by weight) for 48 h to verify the structure of the graphene formed on the talc. Then, the reaction was continued under reflux at 110 °*C* for 3 h in the ratio of by adding 1: 2 = HNO_3: Distilled Water (by volume) to the HF solution that was previously mixed for 48 h. The solution, which was brought to room temperature after the reaction, was centrifuged with distilled water 3 times at 10000 rpm for 30 min. After that the following tests were performed on the synthesised graphene FTIR, XRD, TGA, Raman, SEM, Tensile tests, and XPS.

2.2.4. Validation of reference case test results with previously published results

The laboratory test results given in Table 3 have shown significant similarities to previously published results, enabling the study to move forward to the next stage of graphene use.

2.3. Aggregate and asphalt mix design for reference case

In advance of testing use of graphene, it is intended to conduct tests at laboratory environment for typical Marshall l Mix design [25] in order to enable comparative analysis of graphene using a number of tests such as gradation, mix design, repeat load test, static load test (creep), cohesion and indirect tensile test.
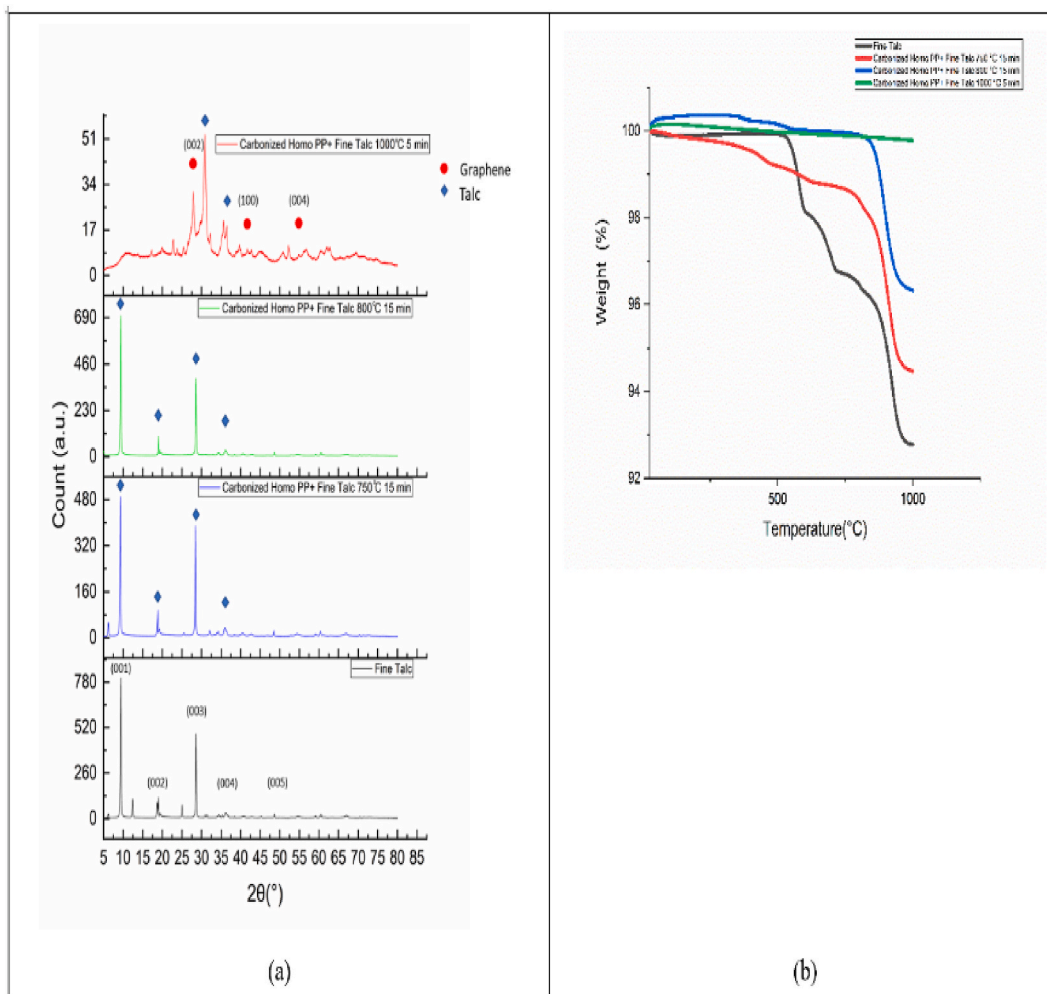
Fig. 6. (a) XRD patterns and (b) TGA curves of Fine talc, Carbonised %20 fine talc + homo PP at different temperatures and heating durations.

Table 1
Asphalt binder properties 40-50.

Property	Values
Penetration 25 °C, 100 gm, 5 s, 0.1 mm	44.0
Softening point (°C)	57.0
Ductility 25 °C, 5 cm/min, (cm)	>100
Specific gravity	1.043
Absolute viscosity 60 °C (poise)	4073
Kinematics viscosity 135° CSt	476
Loss in weight %	0.344 %
Residual permeability after	58
Loss	35
Solubility in solution (CCl$_4$)	99.3 %

2.4. Properties of the materials used

2.4.1. Gradation system by penetration

The Penetration test includes measuring the amount of penetration in units of 0.1 mm that a standard needle makes to a sample of solid asphalt under the influence of a load measuring 100 g for a measurement time of 5 s and at a standard temperature of 25°C. According to the American Standard Specifications, the asphalt is divided into five sections: A/40–50. B/60–70. C/85–100. D/120–150. E/200–300 (ASTM D946M). Size reduction to 0.1 mm. The lower the degree of insertion in the asphalt, the denser it is.

Table 2

The Physical properties of graphene.

Physical characteristics	Value
Purity	>98 wt%
Scale	<8 nm
Lamellar size	8–60 μm
Numbers of graphene layers	8–10
Electrical Conductivity	>1200 S/m
Oxygen content	0.5 %
Content of mineral impurities	85 ppm
Specific surface area	105–135 m2/g

Table 3

A comparison of raw graphene results from previous studies [25] with the current study.

Physical characteristic	current study	previous study [25]
Purity	>98 wt%	>95 wt%
Scale	<8 nm	<6 nm
Lamellar size	8–60 μm	6–50 μm
Numbers of graphene layers	8–10	6–10
Electrical Conductivity	>1200 S/m	>1100 S/m
Oxygen content	0.5 %	0.5 %
Sulphur content	0.5 %	0.5 %
Content of mineral impurities	85 ppm	65 ppm
Specific surface area	105–135 m^2/g	95–115 m^2/g

Asphalt 200–300 is the framework of the types of asphalt and is used in cold regions such as Canada. Asphalt 60–70 is used in flexible paving works in countries such as the Republic of Egypt, Sudan, and United Arab Emirates which is suitable for its air temperature. Asphalt 40–50 is the standard used semi-hot areas such as Mediterranean Countries; Türkiye, and the Turkish Republic of Northern Cyprus (TRNC) where this study is conducted.

The aggregate used in this study is crushed aggregate obtained from one of the asphalt paving production plants in Kocaeli city, in addition to the use of cement as a filler. Laboratory tests were conducted to find and evaluate the physical properties of the aggregate (coarse and fine) necessary to determine the possibility of using it in the hot asphalt mixture and according to the requirements of the Turkish specification (ASTM D946M) and for roads and bridges, as the quality of the aggregate is an important factor in the performance of paving, as shown in Table 4.

2.4.2. Asphalt mix design

The Marshall l method was used to find the ideal content of asphalt and to prevent the movement of particles of aggregates resulting from the increase of the asphalt content. This method is one of the most common methods used and approved by most of the design authorities. Marshall l cylindrical models were used in this examination, with dimensions of 6.101 mm in diameter and 5.63 mm in height. The stability and creep were checked according to the test method described in specification [1559-D-ASTM], using a Marshall l device to calculate stability and creep.

2.5. Testing

2.5.1. Repeated load test

This test was conducted to find the modulus of elasticity necessary to evaluate the performance of the asphalt mixture used in the surface layer of the asphalt in this study. The repeated axial load test was carried out using a device that provides a repeating load system and using cylindrical Marshall l Models for asphalt mixture. The load test is carried out according to specification 4123-ASTM-D and by applying a radial repetitive stress load on the model with a load succession time of 0.1 s and a loading period of 0.9 s. No rest period, stress levels 6.5 and 13 pounds per square inch and three temperature levels of 10, 25 and 40 °C were used. The vertical

Table 4

Aggregate physical properties.

Property	Test result
The total specific weight of the coarse aggregate	2.663
Apparent specific weight of coarse aggregate	2.705
Water absorption ratio of coarse aggregate	0.57 %
The total specific gravity of fine aggregate	2.531
Percentage of degraded aggregate crushing Los Angeles examination max 30 %	22 %
Crushing ratio min 95 %	99 %

deformation that occurred under different load frequencies was measured during the examination.

The following procedures are performed:

1. The model is left for 2 h at the required examination temperature to ensure uniform temperature distribution in the model.
2. The form is placed inside the examination apparatus, after pre-determining all the examination conditions such as pressure, loading periods, lifting the specified load and regulating the temperature used for examination.
3. A high-resolution video camera (14X zoom) is operated, placed in a suitable place in front of the reading display device. This is connected to the examination device, which starts displaying the readings as soon as the examination begins.
4. The test begins by shedding repeated stress in the form of repeated pulses (cycles) of load and no load and return at each pulse of load and no load. The device reads the recovered elastic deformation.

2.5.2. Static load test (creep)

The models used for this examination are Marshall l test models using the ideal content of asphalt in the asphalt mixture used for the models. This is tested by applying a uniaxial constant load and stress levels of 6.5 and 13 pounds per square inch at a temperature of 25 and 40 °C, the load is applied directly for 50 min and distortion is read. The device used is manufactured to apply a constant load on the models. The experiments are carried out using the recommended minimum standard AASHTO TP 125 of five replicates. The readings for the successive loading times were recorded at: 1, 10, 30, 60, 260, 360, 500, 1000, 2000, and 3000 s.

2.5.3. Cohesion test

The cohesion of the compacted asphalt mixture was found by measuring the force required to break or twist the model by a Hveem
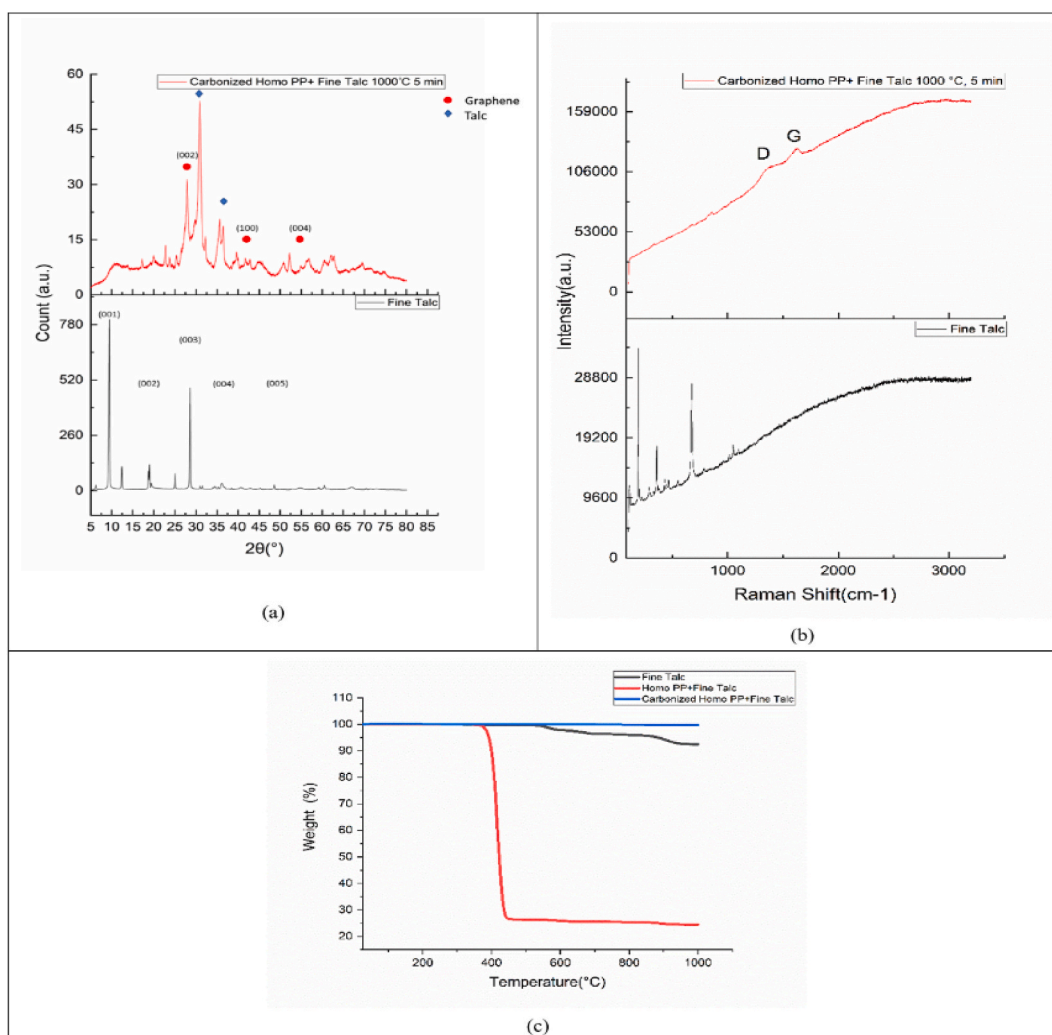

Fig. 7. XRD patterns of (a) fine talc and carbonised graphene/fine talc hybrid (from PP source), Raman spectrum (b) fine talc and carbonised graphene/fine talk hybrid (from PP source), and TGA curves of (c) Fine talc, homo PP+%20 fine talc and carbonised homo PP+%20 fine talc.

cohesiometer. The models used for this examination are Marshall l Models; different ratios were used (4.0 %, 4.5 %, 5.0 %, 5.5 %, 6.0 %) to show the effect of asphalt content on cohesion, as mentioned in specification 1560-ASTM-D. The test temperature is 60 °C, in addition, other temperatures were used to observe the effect of temperature on the cohesion test. The test represents an experimental measurement of internal friction in the model that reflects the properties of aggregate and asphalt, where the strength and stability of the hot asphalt mixture includes cohesion and internal friction.

2.5.4. Indirect tensile test

Indirect tensile testing is very important to understand the tensile strength and to know the amount and shape of failure of the mixture. It represents the highest tensile stress calculated from the highest applied load at failure. In this examination, Marshall l Models with dimensions of 101.6 and 63.5 mm were used for the asphalt mixture at the ideal content of asphalt and for a temperature of 25 °C, i.e. the standard test temperature. Place the bottom and top of the model in the middle along the diagonal of the model. The load is continuously applied in the direction of the diameter and at a constant rate to record the highest value of the load.

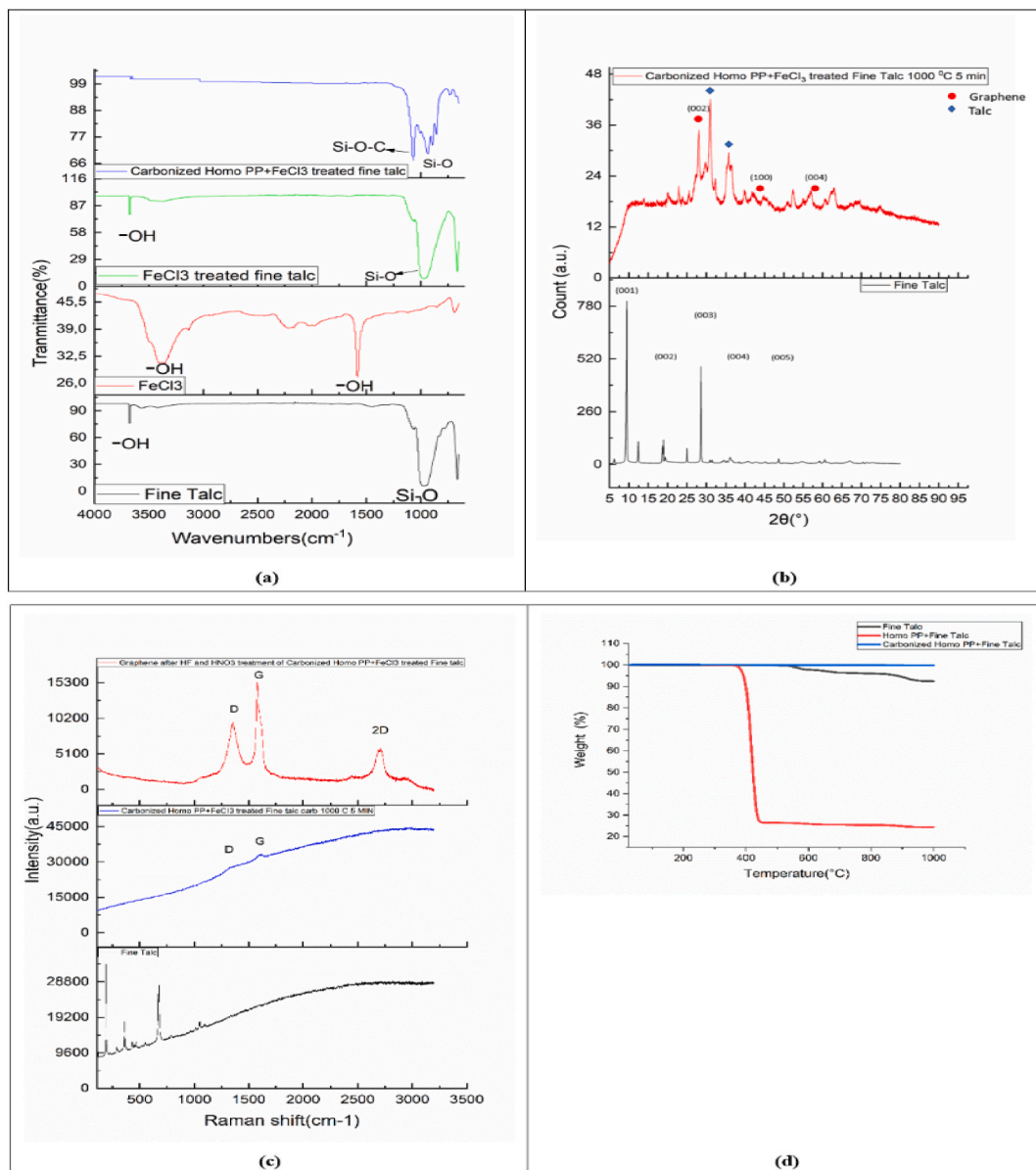**Fig. 8.** (a) FTIR spectrum of Fine talc, FeCl$_3$, FeCl$_3$ treated fine talc, Graphene/Fe-fine talc hybrid after carbonization, (b) XRD patterns of Fine talc and Graphene/Fe-fine talc hybrid, (c) Raman spectrum of Fine talc, Graphene/Fe-fine talc and Graphene separated after acid treatment and (d) TGA curves of Fine talc, homo PP+%20 Fe-fine talc before carbonization, and Graphene/Fe-fine talc hybrid after carbonization.

3. Results and discussion

3.1. Graphene synthesis results

A close look at the usage of thermoplastics filled with talc reveals the fact that graphene/fine talc hybrid was produced from the homo PP (80 %) + talc (20 %) compound after the carbonization at 1000°C within the duration of 5 min. Fig. 7 illustrates XRD patterns, Raman spectrums, and TGA curves of fine talc and carbonised graphene/fine talc hybrid. Whereas it was determined that the peak of graphene which corresponds to the (002) plane was formed in XRD, it was observed that the D and G peaks appeared after the carbonization process in the Raman spectrum. Fig. 7a shows the pattern of fine talc and carbonised graphene with fine talc hybrid, Fig. 7b shows the Raman spectrum fine talc and carbonised graphene with fine talc hybrid from PP source with TGA curves, and Fig. 7c shows fine talc and carbonised graphene at 20 % fine talc. TGA curves elucidates that graphene/fine talc hybrid revealed high thermal resistance. Therefore, these analyses confirm that talc can be used as a substrate for production of graphene.

Synthesised graphene was dried at 80°C for 24 h. Fig. 8 illustrates FTIR, XRD, Raman, and TGA analysis of $FeCI_3$- treated hybrid additive and graphene formation after acid treatment. Fig. 8a illustrates the FTIR spectrum of fine talc, $FeCI_3$, $FeCI_3$ treated fine talc, and graphene/$FeCI_3$ treated fine talc hybrid after carbonization. The FTIR peaks around 987 cm^{-1} and 665 cm^{-1} corresponding to the formation of Si–O and Si–O–Si bindings. Broad peaks are formed at 3359 cm-1 due to occurrence of –OH functional groups, and sharp peaks are formed at 1580 cm-1 due to the occurrence of water molecules that are physically absorbed at the iron surface. The FTIR spectrum of Fe treated talc reveals a distinctive difference in the spectrum. However, at around 1065 cm-1 there is formation of a Si–O–C peak after the carbonization process. This observation indicates that the carbon from Polypropylene was attached to the surface of talc.

Fig. 8b, reveals XRD patterns of fine talc and growth of Graphene/Talc hybrid additive by using carbonised iron metal catalyst. During the carbonization, the main peak of talc that corresponds to the 001 plane has vanished and elevated temperatures result in the complete destruction of crystalline structure of talc and formation of amorphous structure. Small XRD peak at around 43 °C reveals the turbot rain graphene formation. In addition to that, graphene peaked at 25.5 °C which corresponds to the plane of 002 occurring. There was a vast amount of noise peaks in the XRD characterization of the sample, which is treated by acid treatment after the carbonization [37].

The change in the Graphene and carbon structures can be effectively elucidated by Raman Spectroscopy. The graphite has three prominent Raman peaks of 1348 cm^{-1}, 1577 cm^{-1}, and 2715 cm^{-1} which correspond to the D, G, and 2D bands. D band is related to the irregularity caused by defects in the structure and the intensity of the band peak increases with the defect in the structure. On the other hand, G band peak reveals in-plane vibrations of sp2 bonded carbon atoms and peak intensity varies due to differences in the graphene layers.

When D and G peak intensity ratios (ID/IG) increased, that increase elucidates breakage of the sp2 bonds and this resulted in more formation of sp^3 bonds and increase in the amount of the defects in the structure. Fig. 8c, illustrates three prominent sharp Raman peaks of 192 cm^{-1}, 359 cm^{-1}, and 674 cm^{-1}.

However, after carbonization process, talc peaks are vanished and peaks with less intensity at 1321 cm^{-1} and 1596 cm^{-1} and broad D and G band peaks occurred. After performing acid treatment to the hybrids, at 1353 cm^{-1}, 1577 cm^{-1}, and 2703 cm^{-1} intensities of D, G, and 2D band peaks increased and distinct formation of graphene Raman spectrum was observed [38]. Raman characterization results proved that it is possible to produce graphene by using the carbon sources in polypropylene.

Fig. 8d, reveals TGA curves of fine talc, Homo PP+20 % Fe-Fine talc before carbonization and Graphene/Fe-Fine hybrid after the carbonization. Looking at the TGA curve of homo PP + 20 % Fe-fine talc obtained before carbonization, there was a sharp weight loss from 450 °C to 80 % weight loss was observed. On the other hand, a higher thermal stability was observed in the hybrid graphene/talc additive obtained after carbonization at 1000 °C in 5 min compared to both fine talc and its form carbonization before carbonization.

Tensile and flexure test specimens were prepared in accordance with ISO 527-2 and ASTM-D790 with the Explore injection machine for mechanical test analysis of homoPP and copoPP composites prepared with thermokinetic mixer, respectively. Bending and tensile test results of additives produced in presence of untreated micron talc, which is graphene talc reinforcement with untreated talc, has a positive effect on their modulus and strength values [39]. According to the mechanical properties, additive type and additive rate, the highest improvement values are shown in the tables. With 20%-micron talc, whose bending results were examined, 33 % increase in bending strength and 92.7 % increase in bending modulus was achieved. Table 5 lists the characteristics of micron talc

Table 5
Flexural test results of micron talc reinforced homo PP composites.

Specimen name	flexural strength	improvement in flexural strength (%)	flexural modulus (MPa)	Improvement in flexural modulus (%)	flexural strain (%)
HomoPP	46	–	1733	–	6.6
HomoPP + 5 % micron talc	58.9	28.0	2493	43.9	6.0
HomoPP + 1 % 0 μm talc	60.4	31.3	2770	59.8	5.4
HomoPP + 1 % 5 μm tal	61.0	32.6	3080	77.7	5.2
HomoPP + 2 % 0 μm talc	61.2	33.0	3340	98.1	4.9

Flexural tests homopolymer polypropylene of composites

3.2. Sensitivity of asphalt to temperature and asphalt permeability index

The permeability index is a factor to show the sensitivity of asphalt to temperature, for this study it was found using equation (1), which mainly depends on the permeability at 25 °C and the ductility of the used asphalt.

$$P.I. = [30 / (1 + 90K)] - 10 \tag{1}$$

$$K = [(log\ 800 - log\ P(77°F)] / [S.P.(F°) - 77°F]$$

Where:
 P.I, Permeability Index for Asphalt
 S.P: Softness degree of asphalt °F
 P: Standard permeability at 25 °C

Permeability index values range between 2 and 2-, with a value greater than 2 being low sensitive to temperature and a value smaller than 2 being highly sensitive, and between normal sensitivity. The calculated permeability index was 0.0553, showing the asphalt used is naturally sensitive to temperature because the value of the permeability index ranged between 2 and -2.

3.3. Finding the optimum asphalt content

The ideal content of asphalt was calculated by utilising the results of the calculated values for the properties of the Marshall l experiment by taking the average for the following values:

- Asphalt percentage at the highest density.
- Asphalt percentage at the highest stability.
- Asphalt percentage at 4 % air spaces

After taking the average of the three values, the ideal content of asphalt used for the mixture was 5 % of the total weight of the mixture. This percentage represents a normal value for the hot asphalt mixture used to create the smooth gradient surface layer, as the high surface area needs a high percentage of asphalt compared to the percentages needed in the rest of the layers; it has a coarse gradation to enable the aggregate particles to bind together [40]. Table 6 shows the properties of the mixture at the ideal content with the corresponding values of the Turkish and TRNC Standards.

3.4. Testing with and without graphene for modulus of elasticity of the hot mix asphalt

Equation (2) was used to calculate the modulus of elasticity of the hot mix asphalt.

$$\text{Mr} = p(0.27 + v)/(\Delta h)t \tag{2}$$

Where:
 Mr: modulus of elasticity, (Ib\in 2 psi)
 P: maximum applied load, (Ib).
 v: Poisson's ratio (0.35).
 Δh: The horizontal deformation recovered from the model ($\Delta h = \Delta\ v \times v$), (in).
 Δ v: vertical distortion of the model
 t: the height of the model (in).
 The results obtained from this examination showed that the values of elastic modulus:

- It increases with the increase in the applied pressure according to the value of the load resulting from each pressure, as it is directly proportional to the applied load.
- It is inversely proportional to the temperature when the synthetic graphene is present

Table 6
The results of the Marshall l experiment and their characteristics at the ideal asphalt content.

Physical characteristic	Surface Layer Type IIIB 40–50 gradient	Ideal
Optimum asphalt content	5 %	4–6%
Stability KN	11.8	minimum 8
Flow mm	2.4	2–4
Percent air voids	3.8	3–5
Voids in the mineral aggregate VMA %	15.18	minimum 14
Voids full in of Bitumen VFB %	75	65–85

● It is inversely proportional to the proportions of asphalt in the mixture of asphalt with synthetic graphene

The resulting graphs show the influence of each of the factors used to evoke the other, or the influence of two factors to evoke the third. Fig. 9 shows the inverse relationship between the asphalt ratios of the hot asphalt mixture with the synthetic graphene used in the formation of the surface layer for each applied pressure. Figure 9a shows the values of the elastic modulus at a temperature of 10 °C, which shows the significant and obvious difference in the values of the elastic modulus according to the used pressure values, compared to the values of the elastic modulus. Flexibility at 25 °C (Figs. 9b) and 40 °C (Fig. 9c).

In general, when the temperature is kept constant, it is observed that a large difference in the values of the modulus of elasticity for asphalt percentages 4 % with the difference in pressure, and with the increase in the percentage of asphalt with the increase in temperature, this difference decreases and there is a convergence in the values of the elasticity modulus with the difference in pressure, as the effect of pressure decreases with the increase in temperature and becomes the most influential factor on the modulus of elasticity [41].

Addition of synthesised graphene illustrates the effect of temperature variation on the modulus of elasticity values at temperatures according to the percentages of asphalt in the asphalt mixture at pressure 6.5 and 13 pounds/square inch. The asphalt mixture, but with the increase in temperatures, a remarkable convergence of the values of the modulus of elasticity occurs despite the different percentages of asphalt, meaning that the increase in temperature has a greater effect than the effect of the asphalt ratios [42].

3.5. Testing with and without graphene for the static load test (creep)

Through this test, the resistance of the asphalt mixture with synthesised graphene to permanent deformation was found at a temperature of 25 and 40 °C and an applied static load of 6.5 and 13 pounds/sq. The results of this examination include the following characteristics, which are described in Table 7.

1 The total strain (Creep Strain): the strain represents the deformation occurring in the model divided by the thickness of the model. The total strain of the models was calculated using equation (3):

$$\varepsilon p = \frac{Cd * 10^6}{h} \tag{3}$$

Where:
εp: Strain (mm/mm).
Cd: Distortion in the model (axial creep distortion) (mm).
h: Height of the pattern (mm).

2 Creep Stiffness: This is the representation of the relationship between the applied stresses divided by the total strain of the model, it is calculated using equation (4).

Creep Stiffness = applied pressure / total strain $\tag{4}$

3 The creep response Creep compliance equation was used to calculate the value of the resulting crawl response by dividing the strain, as seen in equation (5).
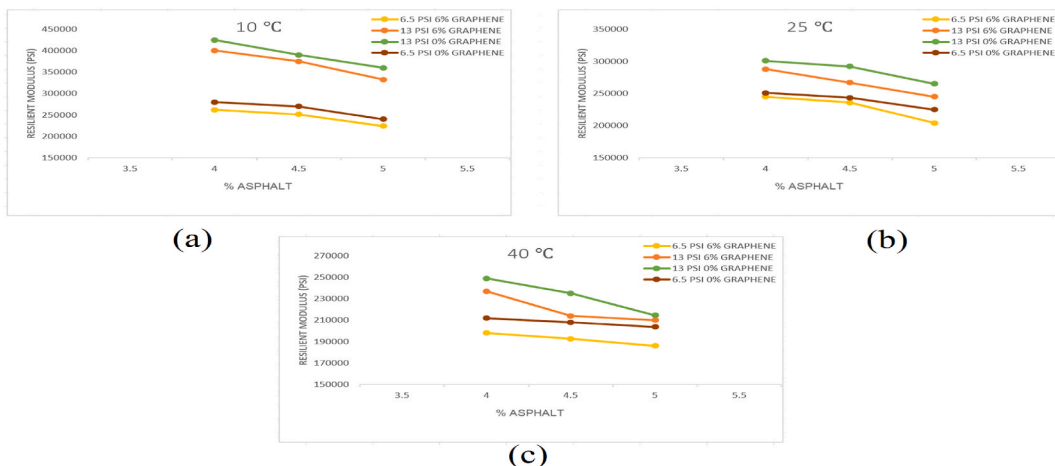

(a)

(b)

(c)

Fig. 9. Effect of the percentage of asphalt in the hot asphalt mixture with 6 % synthesised graphene on the values of the modulus of elasticity according to pressure and at a temperature of (a) 10 °C (b) 25 °C (c) 40 °C.

Table 7
Results of the static load test (static creep).

samples	Kpa	°C	Total strain umm/umm	Creep Stiffness 10^6 Kpa	Creep compliance 10^{-6} Kpa
1	50	25	2634	4.27	11.58
2	50	40	6654	1.63	28.6
3	100	25	10003	2.24	22.05
4	100	40	21148	1.06	45.2

Creep compliance = Strain mm/mm /Applied Stress　　　　　　　　　　　　　　　　　　　　　　　　(5)

Fig. 10a shows the strain that occurred with the examination time for temperatures of 25 and 40 °C with and without synthesised graphene at constant pressure at 6.5 Psi, and 13 Psi in Fig. 10b. Fig. 11 represents the total strain with constant pressure and temperature change, Fig. 11a at 25 °C for each of 6.5 and 13 Psi, and Fig. 11b represents the total strain at 40 °C.

The results showed a clear difference between the values of the total strain for each amount of applied stress and at each temperature used in the examination "with and without" synthesised graphene, as the deformation increase according to the increase in temperature and the applied stress, meaning that the total strain is directly proportional to the temperature and pressure as shown in the Figs. 10 and 11.

The results of the tests showed a clear difference in the internal friction values between the different percentages of asphalt and the temperatures used with and without synthesised graphene. Internal friction increases by increasing the percentage of asphalt and to the maximum. After the maximum, it begins to decrease due to the increase in the percentage of asphalt between the aggregate particles of the mixture. This is because it weakens the cohesion of the aggregate particles causing them to slide.

3.6. Indirect tensile strength test

Equation (6) was used to calculate the tensile strength of the mixture at the highest load causing failure.

$$ITS = \frac{2000p}{\pi Dt}$$ 　　　　　　　　　　　　　　　　　　　　　　　　(6)

Since:
ITS: Indirect tensile strength Kpa
p: highest projected load *KN*
D: the diameter of the pattern, *mm*
t: the thickness of the pattern, *mm*
The average value of the indirect tensile strength of the models used with and without synthesised graphene was 1436 Kpa, this is generally considered to be well tolerated on the asphalt indirect tensile strength scale.

3.7. Testing with and without graphene for cohesion test

The cohesion is inversely proportional to the temperature, and it increases by decreasing the temperature. Cohesion is as high as possible at 25 °C, as the cohesion relationship remains constant from the different percentages of asphalt and at all examination temperatures. The highest and lowest percentage of asphalt are close, especially at a temperature of 60 °C, as shown in Fig. 12. This shows that increasing or decreasing the percentage of asphalt more than the required limit leads to decreased cohesion and internal friction between the aggregates [43,44]. Tables 8–10 show the cohesion test results carried out with 6 % graphene at temperatures of
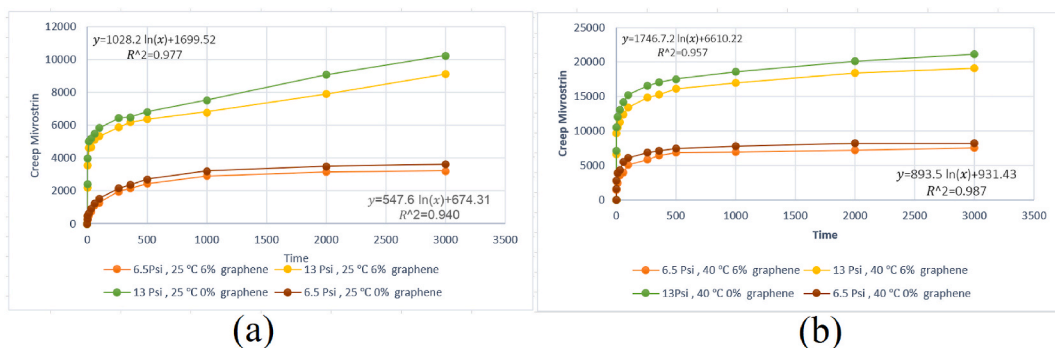

Fig. 10. Illustration of the effect of temperature on the creep with constant pressure (a) under pressure 6.5psi (b) under pressure of 13psi.
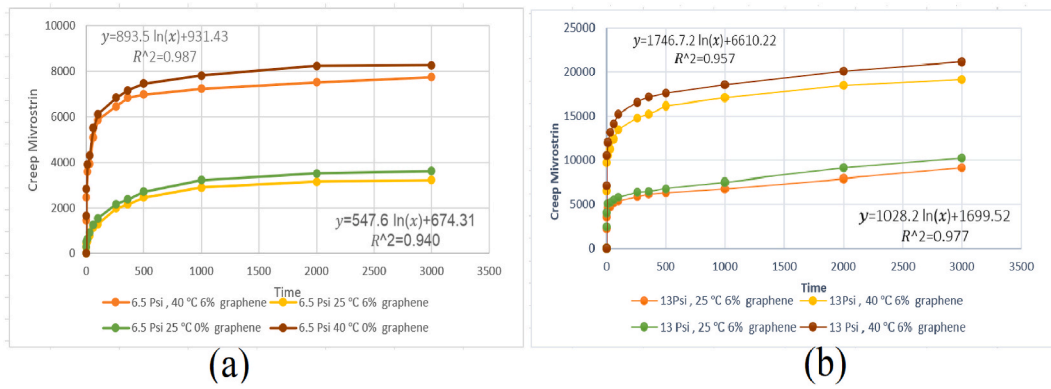
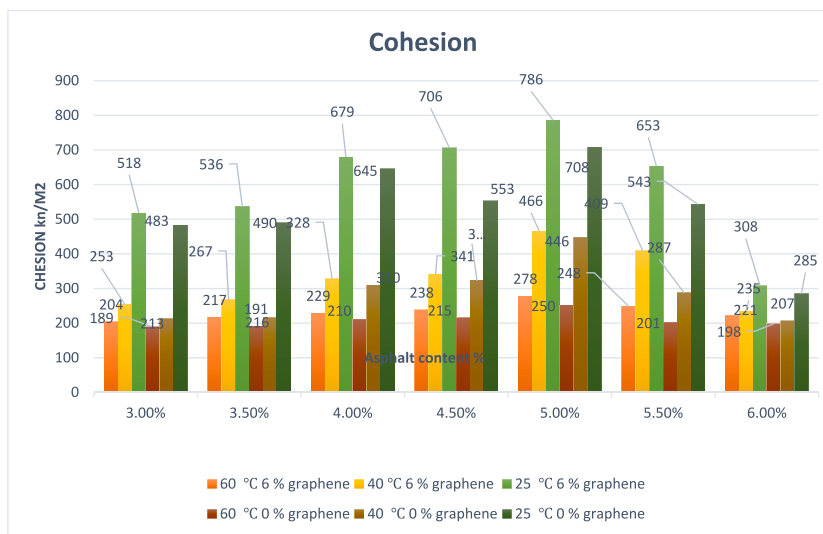**Fig. 11.** Illustration of the effect of pressure applied at constant temperature (a) at 40 °C (b) at 25 °C

Fig. 12. Effect of asphalt percentages on cohesion values and temperatures used with and without synthesised graphene.

Table 8
Cohesion test results with graphene at 6 % and temperature at 25 °C.

asphalt percentages	test 1	test 2	test 3	KN/m2 avg	Standard deviation	Standard deviation error
3.00 %	520	523	511	518	6.244998	3.605551
3.50 %	535	539	534	536	2.645751	1.527525
4.00 %	669	684	684	679	8.660254	5
4.50 %	702	708	708	706	3.464102	2
5.00 %	789	785	784	786	2.645751	1.527525
5.50 %	658	654	647	653	5.567764	3.21455
6.00 %	309	304	311	308	3.605551	2.081666

25 °C, 40 °C, and 60 °C. The peak cohesion is realised at 6 % graphene mixture with 5 % asphalt with 786 Km/M^2. This peak is an average of a total of three experiments carried out with the same parameters.

4. Economic evaluation

Synthesis of graphene was presented in our study entails cost components which include energy consumption, equipment, and raw materials. The raw materials aspect of it in the context of plastic bottles is the primary source of raw materials for the proposed method. Other material costs include equipment and other catalysts and chemicals used in the proposed synthesis process. The proposed method compared to traditional methods of graphene synthesis offers a potential economic savings. This is due to the abundance of discarded plastic bottles which is currently an alarming environmental hazard. The cost efficiency associated with the proposed study

Table 9

Cohesion test results with graphene 6 % and temperature at 40 °C.

asphalt percentages	test 1	test 2	test 3	KN/m2 avg	Standard deviation	Standard deviation error
3.00 %	255	251	253	253	2	1.154701
3.50 %	264	271	266	267	3.605551	2.081666
4.00 %	331	329	324	328	3.605551	2.081666
4.50 %	345	346	332	341	7.81025	4.50925
5.00 %	470	462	466	466	4	2.309401
5.50 %	410	399	418	409	9.539392	5.507571
6.00 %	236	237	232	235	2.645751	1.527525

Table 10

Cohesion test results with graphene 6 % and temperature at 60 °C.

asphalt percentages	test 1	test 2	test 3	KN/m2 avg	Standard deviation	Standard deviation error
3.00 %	205	200	207	204	3.605551	2.081666
3.50 %	215	218	218	217	1.732051	1
4.00 %	230	231	226	229	2.645751	1.527525
4.50 %	239	234	241	238	3.605551	2.081666
5.00 %	277	281	276	278	2.645751	1.527525
5.50 %	244	251	249	248	3.605551	2.081666
6.00 %	222	219	222	221	1.732051	1

also presents an associated environmental sustainability advantage. The proposed method adheres to the concept of upcycling of solid waste which in this study is plastic waste. Hence, the potential economic advantages presented by this proposed study are outlined as follows:

- **Waste Reduction**: Utilising plastic bottle waste for graphene synthesis contributes to waste reduction and landfill diversion, addressing environmental concerns associated with plastic pollution.
- **Resource Efficiency**: By repurposing plastic waste into a valuable material like graphene, the synthesis process enhances resource efficiency and promotes circular economy principles.
- **Cost-Effective Asphalt Modification**: Incorporating graphene synthesised from plastic bottle waste into asphalt mixture offers the potential for cost-effective pavement modification. Graphene additives can improve the mechanical properties, durability, and performance of asphalt, potentially reducing maintenance and repair costs over the pavement lifecycle [47–49].

The cost of production is completely new research and should be further studied to examine the practical costs in production. However, it is also considered that policies to mitigate any additional cost should be imposed to construction techniques not involving recycling and sustainability to create an advantage.

5. Conclusions

This study was carried out to research the use of recycled plastic in the production of asphalt and also to find cost-effective methods for the production of industry-grade graphene. The proposed method as presented in this study has shown the production of high-quality graphene using a mixture with talc, relative to the use of pure graphene. Using the proposed method graphene with a purity level of 98 % was achieved, which is 3 % higher than the raw graphene purity level; of 95 %. The proposed method also results in the synthesis of graphene with 8–10 layers which is higher than the raw graphene with 6–10 layers. The proposed method also shows the best proportion of plastic waste and talc for graphene synthesis is 80 % and 20 % respectively, resulting in graphene with a flexural strength of 61.2 Mpa compared to raw one 46 Mpa. The proposed method shows upcycling of plastic waste and talc mixture produces high-grade graphene. The findings of this study also indicate very good performance characteristics of the synthesised graphene asphalt mixture when compared to asphalt mixture without the use of synthesised graphene from plastic waste. Where the asphalt mixture shows remarkable convergence on the modulus of elasticity occurring with increase in temperatures.

The results of this study show it is possible to upcycle plastic waste into high-grade asphalt pavement construction material. This enables the production of high-grade pavement construction and also ensures sustainable development to mitigate environmental pollution. Production of graphene using plastic waste and talc has the potential of significantly reducing the cost of graphene production which can contribute to meeting the demands of graphene using cost-effective methods. The industrial application of the proposed method can significantly contribute to the recycling and upcycling of plastic waste, leading to the contribution of reducing landfilling and incineration of plastic waste. Research has shown about 300 million tons of plastic waste is generated annually, and only about 36 % is recycled or upcycled [45]. hence, with a global annual production of about 270 million tons of asphalt [46], there is a feasible application of the proposed method in the production of pavement construction material.

6. Future work and recommendations

The proposed methodology in this study has a limitation of asphalt standards limited to only the asphalt 40–50 standard which is applicable to a large number of countries, and certainly in Türkiye, and the Turkish Republic of Northern Cyprus (TRNC) where this study is implemented. However, it is recommended that future studies can be conducted that will consider alternative asphalt standards, and investigate the applicability of the proposed graphene synthesis in this research for asphalt mixture.

Based on the findings of the proposed method, this study recommends the use of synthetic graphene in industrial asphalt mixtures. This study recommends the use of synthesised graphene as presented in this study as high-grade materials, but also to ensure sustainable development, and the protection of the environment. This study also recommends the exploration of the proposed method of synthesising graphene for applications in other industries, such as concrete, electronic device production and other fields.

### Data availability statement

Data will be made available on request

CRediT authorship contribution statement

Abdulrahman Alsaid: Writing – original draft, Methodology, Investigation, Formal analysis, Data curation, Conceptualization. **Goktug Tenekeci:** Supervision.

Declaration of competing interest

[The authors declare that they have no known competing financial interests or personal relationships that could have appeared to influence the work reported in this paper.

Appendix
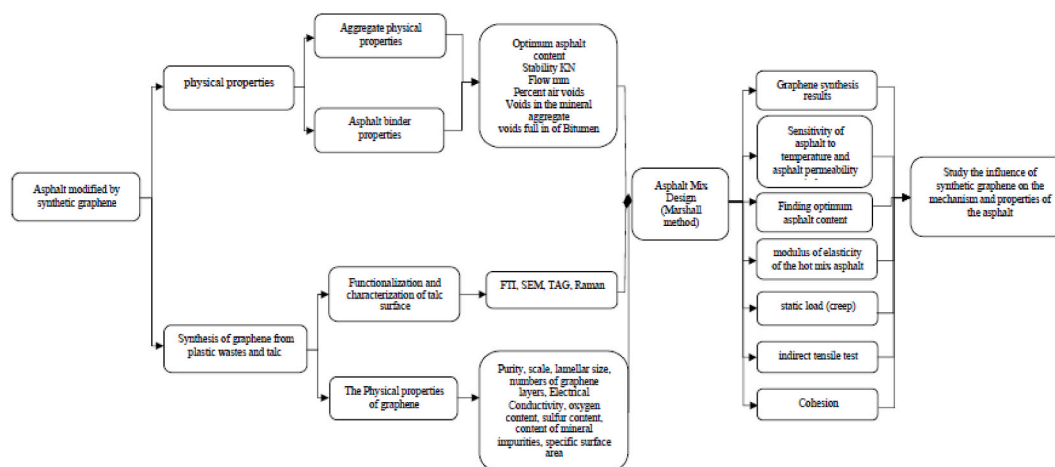
References

[1] Z. Lu, Z.G. Feng, D. Yao, X. Li, X. Jiao, K. Zheng, Bonding performance between ultra-high performance concrete and asphalt pavement layer, Construct. Build. Mater. 312 (2021) 125375.

[2] A. Alatawna, M. Birenboim, R. Nadiv, M. Buzaglo, S. Peretz-Damari, A. Peled, R. Sripada, The effect of compatibility and dimensionality of carbon nanofillers on cement composites, Construct. Build. Mater. 232 (2020) 117141.

[3] X. Yan, D. Zheng, H. Yang, H. Cui, M. Monasterio, Y. Lo, Study of optimizing graphene oxide dispersion and properties of the resulting cement mortars, Construct. Build. Mater. 257 (2020) 119477.

[4] I. Rhee, J.S. Lee, Y.A. Kim, J.H. Kim, J.H. Kim, Electrically conductive cement mortar: incorporating rice husk-derived high-surface-area graphene, Construct. Build. Mater. 125 (2016) 632–642.

[5] M. Wang, H. Yao, R. Wang, S. Zheng, Chemically functionalized graphene oxide as the additive for cement–matrix composite with enhanced fluidity and toughness, Construct. Build. Mater. 150 (2017) 150–156.

[6] S. Chuah, Z. Pan, J.G. Sanjayan, C.M. Wang, W.H. Duan, Nano reinforced cement and concrete composites and new perspective from graphene oxide, Construct. Build. Mater. 73 (2014) 113–124.

[7] J. He, W. Hu, R. Xiao, Y. Wang, P. Polaczyk, B. Huang, A review on Graphene/GNPs/GO modified asphalt, Construct. Build. Mater. 330 (2022) 127222.

[8] T. Qureshi, G. Wang, S. Mukherjee, M.A. Islam, T. Filleter, C.V. Singh, D.K. Panesar, Graphene-based anti-corrosive coating on steel for reinforced concrete infrastructure applications: challenges and potential, Construct. Build. Mater. 351 (2022) 128947.

[9] A.G. Alex, A. Kedir, T.G. Tewele, Review on effects of graphene oxide on mechanical and microstructure of cement-based materials, Construct. Build. Mater. 360 (2022) 129609.

[10] J. Huang, Y. Liu, Y. Muhammad, J.Q. Li, Y. Ye, J. Li, R. Pei, Effect of glutaraldehyde-chitosan crosslinked graphene oxide on high temperature properties of SBS modified asphalt, Construct. Build. Mater. 357 (2022) 129387.

[11] M. Han, Y. Muhammad, Y. Wei, Z. Zhu, J. Huang, J. Li, A review on the development and application of graphene based materials for the fabrication of modified asphalt and cement, Construct. Build. Mater. 285 (2021) 122885.

[12] M. Moradi, M. Rezaei, Construction of highly anti-corrosion and super-hydrophobic polypropylene/graphene oxide nanocomposite coatings on carbon steel: experimental, electrochemical and molecular dynamics studies, Construct. Build. Mater. 317 (2022) 126136.

[13] T.P. Ngo, Q.B. Bui, N.T. Nguyen, T. Le, V.T.A. Phan, Application of nanotechnology for earth materials: an exploratory study with graphene-based nanosheets, Construct. Build. Mater. 324 (2022) 126677.

[14] Y. Yao, Z. Zhang, H. Liu, Y. Zhuge, D. Zhang, A new in-situ growth strategy to achieve high performance graphene-based cement material, Construct. Build. Mater. 335 (2022) 127451.

[15] Y. Yao, Z. Zhang, H. Liu, Y. Zhuge, D. Zhang, A new in-situ growth strategy to achieve high performance graphene-based cement material, Construct. Build. Mater. 335 (2022) 127451.

[16] Q. Chen, C. Wang, Z. Qiao, T. Guo, Graphene/tourmaline composites as a filler of hot mix asphalt mixture: preparation and properties, Construct. Build. Mater. 239 (2020) 117859.

[17] P. Yong, J. Tang, F. Zhou, R. Guo, J. Yan, T. Yang, Performance analysis of graphene modified asphalt and pavement performance of SMA mixture, PLoS One 17 (5) (2022) e0267225.

[18] S. Li, W. Xu, F. Zhang, H. Wu, P. Zhao, Effect of graphene oxide on the low-temperature crack resistance of polyurethane–SBS-modified asphalt and asphalt mixtures, Polymers 14 (3) (2022) 453.

[19] Q. Zeng, Y. Liu, Q. Liu, P. Liu, Y. He, Y. Zeng, Preparation and modification mechanism analysis of graphene oxide modified asphalts, Construct. Build. Mater. 238 (2020) 117706.

[20] J. Zhu, K. Zhang, K. Liu, X. Shi, Adhesion characteristics of graphene oxide modified asphalt unveiled by surface free energy and AFM-scanned micro-morphology, Construct. Build. Mater. 244 (2020) 118404.

[21] R. Wang, Z. Qi, R. Li, J. Yue, Investigation of the effect of aging on the thermodynamic parameters and the intrinsic healing capability of graphene oxide modified asphalt binders, Construct. Build. Mater. 230 (2020) 116984.

[22] Y. Wei, Y. Liu, Y. Muhammad, S. Subhan, F. Meng, D. Ren, J. Li, Study on the properties of GNPs/PS and GNPs/ODA composites incorporated SBS modified asphalt after short-term and long-term aging, Construct. Build. Mater. 261 (2020) 119682.

[23] Y. Wei, C. Hu, Y. Muhammad, L. Chen, D. Zhou, S. Wang, Q. Chen, Fabrication and performance evaluation of aminopropyl triethoxysilane-dopamine-MoS2 incorporated SBS modified asphalt, Construct. Build. Mater. 265 (2020) 120346.

[24] J. Liu, P. Hao, Z. Dou, J. Wang, L. Ma, Rheological, healing and microstructural properties of unmodified and crumb rubber modified asphalt incorporated with graphene/carbon black composite, Construct. Build. Mater. 305 (2021) 124512.

[25] X. Li, Y.M. Wang, Y.L. Wu, H.R. Wang, M. Chen, H.D. Sun, L. Fan, Properties and modification mechanism of asphalt with graphene as modifier, Construct. Build. Mater. 272 (2021) 121919.

[26] G. Huang, J. He, X. Zhang, M. Feng, Y. Tan, C. Lv, Z. Jin, Applications of Lambert-Beer law in the preparation and performance evaluation of graphene modified asphalt, Construct. Build. Mater. 273 (2021) 121582.

[27] J.K. Saha, A. Dutta, A review of graphene: material synthesis from biomass sources, Waste and Biomass Valorization (2022) 1–45.

[28] T. Guo, H. Fu, C. Wang, H. Chen, Q. Chen, Q. Wang, A. Chen, Road performance and emission reduction effect of graphene/tourmaline-composite-modified asphalt, Sustainability 13 (16) (2021) 8932.

[29] J. Huang, Y. Liu, S. Subhan, X. Quan, H. Zhong, J. Li, Z. Zhao, Fast deposition of Fe3+ chelated tannic acid network via salt induction over graphene oxide based SBS modified asphalt, Construct. Build. Mater. 307 (2021) 125009.

[30] X. Li, Y. Wang, Y. Wu, H. Wang, Q. Wang, X. Zhu, L. Fan, Effect of graphene on modified asphalt microstructures based on atomic force microscopy, Materials 14 (13) (2021) 3677.

[31] Y. Chen, Q. Wang, Z. Li, S. Ding, Rhysiological properties of graphene nanoplatelets/rubber crowd composite modified asphalt, Construct. Build. Mater. 261 (2020) 120505.

[32] A.M. Adnan, X. Luo, C. Lü, J. Wang, Z. Huang, Improving mechanics behavior of hot mix asphalt using graphene-oxide, Construct. Build. Mater. 254 (2020) 119261.

[33] F. Moreno-Navarro, M. Sol-Sánchez, F. Gámiz, M.C. Rubio-Gámez, Mechanical and thermal properties of graphene modified asphalt binders, Construct. Build. Mater. 180 (2018) 265–274.

[34] Y. Li, S. Wu, S. Amirkhanian, Investigation of the graphene oxide and asphalt interaction and its effect on asphalt pavement performance, Construct. Build. Mater. 165 (2018) 572–584.

[35] M. Han, J. Li, Y. Muhammad, D. Hou, F. Zhang, Y. Yin, S. Duan, Effect of polystyrene grafted graphene nanoplatelets on the physical and chemical properties of asphalt binder, Construct. Build. Mater. 174 (2018) 108–119.

[36] J. Li, M. Han, Y. Muhammad, Y. Liu, S. Yang, S. Duan, Z. Zhao, Comparative analysis, road performance and mechanism of modification of polystyrene graphene nanoplatelets (PS-GNPs) and octadecyl amine graphene nanoplatelets (ODA-GNPs) modified SBS incorporated asphalt binders, Construct. Build. Mater. 193 (2018) 501–517.

[37] K. Liu, K. Zhang, X. Shi, Performance evaluation and modification mechanism analysis of asphalt binders modified by graphene oxide, Construct. Build. Mater. 163 (2018) 880–889.

[38] A. Razaq, F. Bibi, X. Zheng, R. Papadakis, S.H.M. Jafri, H. Li, Review on graphene-, graphene oxide-, reduced graphene oxide-based flexible composites: from fabrication to applications, Materials 15 (3) (2022) 1012.

[39] D. Wang, A. Baliello, L. Poulikakos, K. Vasconcelos, M.R. Kakar, G. Giancontieri, A.C. Falchetto, Rheological properties of asphalt binder modified with waste polyethylene: an interlaboratory research from the RILEM TC WMR, Resour. Conserv. Recycl. 186 (2022) 106564.

[40] C. Xue, H. Gao, G. Hu, Viscoelastic and fatigue properties of graphene and carbon black hybrid structure filled natural rubber composites under alternating loading, Construct. Build. Mater. 265 (2020) 120299.

[41] J. Büchner, D. Ryś, S. Trifunović, M.P. Wistuba, Development and application of asphalt binder relaxation test in different dynamic shear rheometers, Construct. Build. Mater. 364 (2023) 129929.

[42] L. Cheng, L. Zhang, X. Liu, F. Yuan, Y. Ma, Y. Sun, Evaluation of the fatigue properties for the long-term service asphalt pavement using the semi-circular bending tests and stereo digital image correlation technique, Construct. Build. Mater. 317 (2022) 126119.

[43] G. Guo, H. Gong, L. Cong, F. Yang, Laboratory investigation on the cracking performance of paving polyurethane mixture using semi-circular bending test, Construct. Build. Mater. 341 (2022) 127795.

[44] K. Hu, C. Yu, Q. Yang, Z. Li, W. Zhang, T. Zhang, Y. Feng, Mechanistic study of graphene reinforcement of rheological performance of recycled polyethylene modified asphalt: a new observation from molecular dynamics simulation, Construct. Build. Mater. 320 (2022) 126263.

[45] G. Gourmelon, Global plastic production rises, recycling lags, Vital Signs 22 (2015) 91–95.

[46] J. Zhang, Z. Yao, K. Wang, F. Wang, H. Jiang, M. Liang, G. Airey, Sustainable utilization of bauxite residue (Red Mud) as a road material in pavements: a critical review, Construct. Build. Mater. 270 (2021) 121419.

[47] S. Qaidi, Y. Al-Kamaki, I. Hakeem, A.F. Dulaimi, Y. Özkılıç, M. Sabri, V. Sergeev, Investigation of the physical-mechanical properties and durability of high-strength concrete with recycled PET as a partial replacement for fine aggregates, Front. Mater. 10 (2023) 1101146.

[48] J. Ahmad, A. Majdi, A. Babeker Elhag, A.F. Deifalla, M. Soomro, H.F. Isleem, S. Qaidi, A step towards sustainable concrete with substitution of plastic waste in concrete: overview on mechanical, durability and microstructure analysis, Crystals 12 (7) (2022) 944.

[49] A. Dulaimi, S. Qaidi, S. Al-Busaltan, A. Milad, M. Sadique, M.A. Kadhim, M.M. Sabri Sabri, Application of paper sludge ash and incinerated sewage ash in emulsified asphalt cold mixtures, Front. Mater. 9 (2023) 1074738.

[50] A. Kocanalı, H. Baskan-Bayrak, Y. Menceloglu, B. Saner Okan, A selective upcycling approach: growing 2D and 3D graphene oxide structures with size-controlled talc substrates from waste polypropylene with LCA protocols, J. Polym. Environ. 31 (9) (2023) 4052–4068.